Creep-Fatigue Crack Growth in Power Plant Components

F. Bassi[1], S. Beretta[1], A. Lo Conte[1], M. Cristea[2]
[1] Politecnico di Milano, Department of Mechanical Engineering, via Giuseppe La Masa 1, I-20156, Milan, Italy.
[2] Tenaris Dalmine, R&D, I-24044 Dalmine, Italy

Contact data
E-mail address: federico.bassi@polimi.it (F. Bassi)

Summary
In components operating at high temperature, the presence of defect, that may derive from manufacturing process or operating under critical conditions, could raise to creep-fatigue crack growth even at low loading conditions. Creep-fatigue experimental tests have been performed on P91 material, at 600 °C according to ASTM E2760-10 standard, with focus on the effects of the initial nominal stress intensity factor range, ranging between 16 and 22 MPa $m^{0.5}$, and the hold time, ranging between 0.1 and 10 hours. The results will be presented in the paper, together with their application for residual life prediction of a power plant cracked pipe, as case study.

Key Words
Creep, creep-fatigue, crack growth, pipe, residual life assessment.

Introduction
In pressure vessels and piping, the presence of defects due to manufacturing processes or service under extreme conditions, could raise to creep-fatigue crack growth even at non-critical load conditions. The interaction phenomena, between the time-dependent creep damage accumulated during the hours at sustained load (hold time), and the fatigue damage experienced by the material during the scheduled shutdown/startup events (unloading/loading cycles), is a key factor that, at the state-of-the-art, is possible to experimentally address, with laboratory tests performed on the component material, with the aim to introduce dedicated assessment procedures [1].

High temperature fracture mechanics provides a useful framework to design and assess the remaining-life under these conditions. The C_t integral, defined in [2] as the generalization of the stress power dissipation rate interpretation of the C^*-integral, is the appropriate crack tip parameter, to describe the small-scale/extensive creep transition obtained each time a cyclic load is applied. To account for the relevant phenomenon of interaction between the creep damage accumulation at the crack tip and the subsequent effect given by the fatigue cycle, Saxena and Gieseke [3] suggested to represent the driving force of the creep-fatigue crack propagation with an averaged value of the crack tip parameter C_t evaluated at the hold time, the $(C_t)_{avg}$ parameter.

Under creep-fatigue conditions, the stress field at the crack tip is characterized by elastic, plastic, creep, and cyclic plastic zones, that change at each fatigue cycle. While the plastic zone is expected to grow together with crack propagation due to stress increment, the creep zone is expected to increase together with time. The cyclic plastic zone, instead, is expected to stabilize, after a significant number of fatigue cycles. The creep zone size is in continuous competition with the cyclic plastic zone, and their size and evolution depend on both material creep and cyclic plasticity resistance. Between the two limit conditions represented by a dominant creep zone with no creep strain reversed by the fatigue cycle and dominant cyclic plastic zone with creep strain completely reversed by the fatigue cycle, actual materials exhibit instead a partial reverse of the creep strain due to cyclic load. Grover [4] found a correlation between the quantity of reversed creep and the creep reversal parameter C_R, defined as the ratio between the load-line deflection variation calculated at the end of one hold cycle and the beginning of the next hold cycle, and the load-line deflection measured during hold time during creep-fatigue experimental tests. The creep reversal parameter represents an index of the interaction level between the creep and the cyclic plastic zones. An analytical estimation of the $(C_t)_{avg}$ parameter, valid for specimens and components, can be based on this material

index. Experimental correlations of creep-fatigue crack growth rates with $(C_t)_{avg}$ parameter allow then the estimation of the creep-fatigue crack propagation on components.

In power generation and petrochemical plants components operating at high temperature, the creep strength enhanced high chromium steel of ASTM, Grade P91, together with its modifications P911, P92, P122, [5, 6, 7], are the material of widespread interest. In the present work, the material under investigation is a modified P91 grade steel, manufactured by Tenaris for piping applications in steam-cycle boilers at the service temperature of 600 °C. The target of the experimental tests is the study of the effects of the initial nominal stress intensity factor amplitude, as well as the hold time, in the range of interest for the selected application, in order to investigate the creep-fatigue damage interaction and accumulation.

This study provides:

1) a deep characterization of the interaction, at microstructural level, between the voids growth and coalescence during the hold time, and the subsequent fatigue cycle;

2) an experimental calculation of the creep reversal parameter C_R proposed by Grover and Saxena [8], to model the continuous reinstate of the creep strain at the crack tip after each unload/reloading sequence.

3) an experimental correlation between crack growth rates and the average value of the time-dependent crack tip parameter Ct, according to [2];

These results will be presented in the paper, together with their application for a residual life prediction of a power plant cracked pipe.

Material and Creep-fatigue tests

The chemical composition of the examined P91 Grade steel according to ASTM A355 [9] is reported in Table 1 while tensile and secondary creep properties at the tests temperature are summarized in Table 2. In particular, the linear trend of the secondary creep strain rate as function of the stress in a logarithmic plot, presents a variation of the slope at about 120 MPa. Below this stress threshold the Norton exponent is about 4 while above this threshold, when dislocation creep is operative, is about 16 [10]

Creep-fatigue experimental tests (CFCG) have been performed according to the ASTM E2760-10 standard [11], using a SATEC JE 1016 machine, with three controlled zones furnace (Figure 1 a), on ½ inch thickness CT specimens directly machined from a piping component.

Table 1: Chemical composition of the P91 Grade steel [9].

C	Si	Mn	P	S	Al	Cr	Mo	Ni	V	N
0.08-0.12	0.2-0.5	0.3-0.6	<0.02	<0.01	<0.04	8-9.5	0.85-1.05	<0.4	0.18-0.25	0.03-0.07

Table 2: Tensile and secondary creep properties.

T [°C]	Young's modulus [MPa]	Yield stress [MPa]	Norton exponent (n)	
			Low stress	High stress
600	147016	295	4	16

The specimens were pre-cracked at room temperature to obtain a sharp starter crack, and side-grooved to obtain a straight initial crack front, necessary for the subsequent crack validation measurements. The temperature of the specimen was constantly monitored through a S-type thermocouple located in proximity of the specimen notch, while

the furnace controller guaranteed a maximum temperature fluctuation of ±2 °C. The load-line displacement was measured by means of an LVDT extensometer, properly connected by a dedicated equipment. The CT geometry (Figure 1 b) was designed to allow the potential drop crack size measurements. Two holes, in the upper and lower surface, hold the leads that distribute current to the specimen. Four holes, located in the front face of the CT specimen, hold the leads that measure the potential drop in two different zones, remote and local with respect to the crack tip. An experimental calibration curve, for this specific geometry of the specimen, was used to accurately calculate the crack length during the test.

The test machine was equipped with a brushless motor to apply the trapezoidal shaped load history of Figure 1 c). A potential drop measurement, at the beginning of each hold time, was performed to calculate the related crack growth rate. Moreover during the hold time, ten measurements of the load-line displacement have been acquired, to calculate the creep reversal parameter (Figure 1 d).

The CFCG test matrix is reported in Table 3, comprehending the nominal stress intensity factor amplitude ΔK_0, at the beginning of the test, the maximum stress intensity factor at the beginning of the test, $K_{\text{max},0}$, the initial crack size a_0. The load ratio $R = P_{\text{max}}/P_{\text{min}}$ is fixed to 0.1 while the initial nominal stress intensity factor amplitude, ranges between 16 and 22 MPa m$^{0.5}$, and the hold time t_{h} changes between 0.1 and 10 hours.

After each test, specimens were brittle broken in liquid nitrogen for the five crack validation measurements as disposed by the ASTM E2760 standard [9] and as reported in Figure 2 for the specimen tested at $\Delta K_0 = 15.6$ MPa m$^{0.5}$ and hold time = 2h.

Crack Tip Damage

At the end of the CFCG tests, each specimen was sectioned at the midline section, and etched, in order to characterize the evolution of the damage mechanisms, by means of scanning electron microscopy (SEM), with detailed micrographs of the crack front section. The micrographs related to creep-fatigue tests performed at the same value of $\Delta K_0 = 21$ MPa m$^{0.5}$ and different hold times,0.1 h, 1 h, and 10 h, are reported in Figure 3.

The fracture mechanisms result in an irregular shaped inter-granular path typical of creep damage. For short hold time tests (t_{h} = 0.1, 1 h), where the cyclic damage is dominant, the crack profile is characterized by higher peaks and valleys compared to the test with 10 hours hold time. However, in all cases, secondary cracks, branching from the main crack, are present along the crack front (Figure 3 a). As shown in Figure 3 b); a contribution of the oxidation to time-dependent crack growth is present for 1h and 10 hours hold time, with blunted oxidation spikes observed even at the secondary crack tips. As expected, oxidation level is significantly lower for 0.1 h hold time. The relative influence of the environmental effect, on the time-dependent creep-fatigue crack growth, demands for further investigation, in particular when the optimization of the chemical composition of the alloy to improve the high temperature performances is considered. The observation of Figure 3 c) clearly shows, for the considered hold time, the mechanism of fracture starting with voids concentration at the grain boundaries that coalesce, originating creep micro-cavities, and at long terms, intergranular macrocracks. It is evident that the creep deformation and cavitation plays a dominant role in the creep-fatigue crack initiation and growth, while the cyclic load interacts with the creep phenomena at two different levels:

1) at the level of damage mechanism, because generates at the crack tip a wave of damage confined to the cyclic-plastic zone enhancing the hold time creep damage;

2) at the level of microcracks growth, promoting the link between microcracks resulting in secondary cracks and in a faster creep-fatigue primary crack propagation with respect to the pure creep crack growth [10].

At the same value of $\Delta K_0 = 21$ MPa m$^{0.5}$, the more irregular crack profile observed for hold time equal 0.1 h with respect to the profile observed for hold time equal to 10 h, highlights the action of the cyclic load in microcracks linking.

Table 3: Creep-fatigue crack growth tests matrix.

Specimen	R	P_{max} [N]	t_h [h]	ΔK_0 [MPa $\sqrt{m}$]	$K_{max,0}$ [MPa $\sqrt{m}$]	a_0 [mm]
P91-26	0.1	8714	0.1	22.6	25.11	7.99
P91-06	0.1	4750	0.1	21.5	23.88	12.17
P91-137-09	0.1	4435	1	21.2	23.55	12.64
P91-137-10	0.1	4730	10	21.7	24.11	12.31
P91-137-01	0.1	3615	1	16.4	18.22	12.22
P91-07	0.1	3530	2	15.6	17.33	11.99

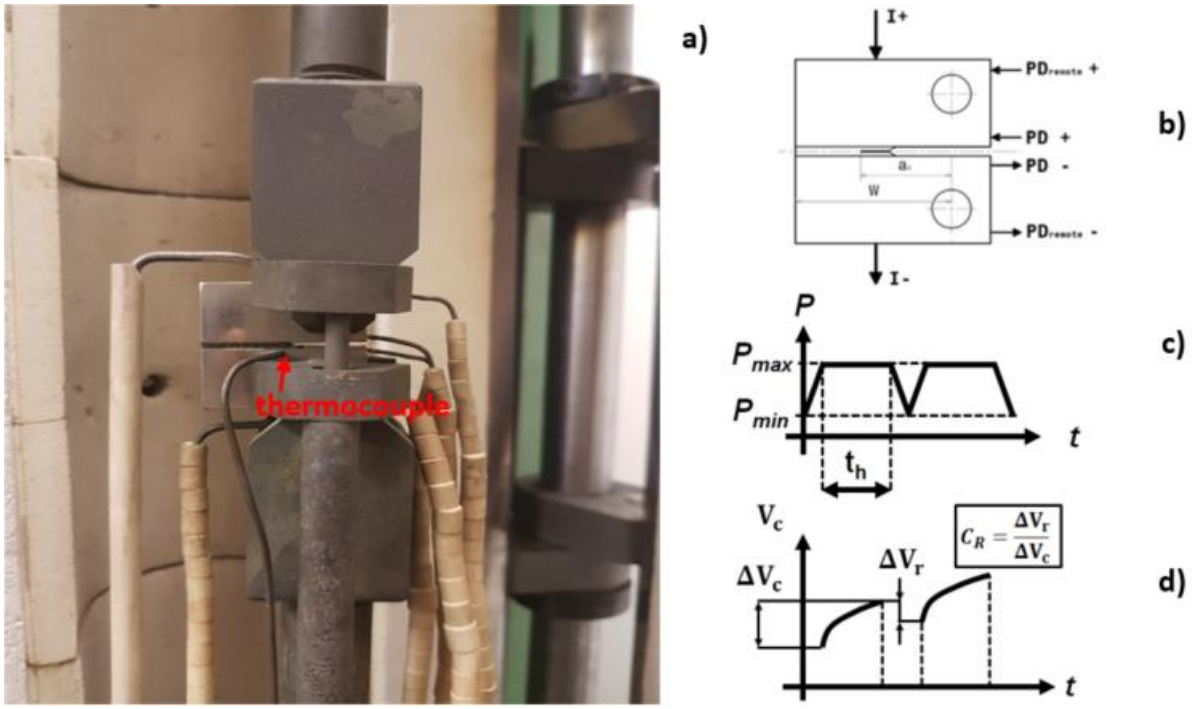

Figure 1: a) Test setup. b) CT specimens with Potential Drop leads configuration. c) Trapezoidal shaped load history. d) Schematic diagram for creep reversal parameter, C_R, determination.

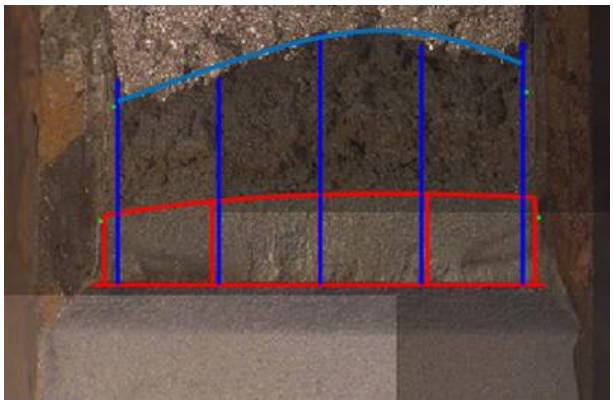

Figure 2: Pre-crack and creep-fatigue crack growth of specimen tested at $\Delta K_0 = 21.7\ MPa\ m^{0.5}$, $t_h = 10\ h$.

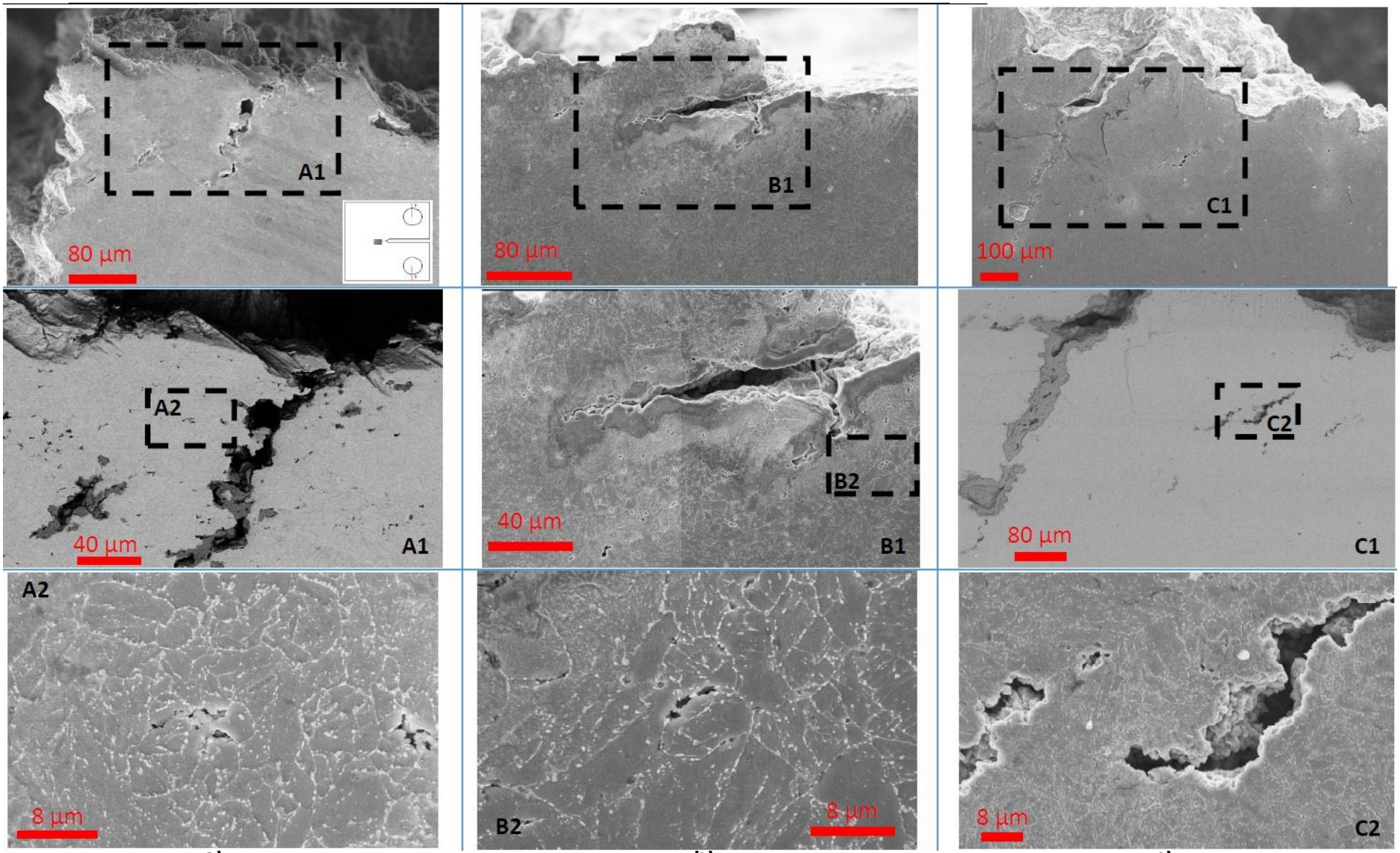

Figure 3: SEM observation of the crack tip damage at $\Delta K_0 = 21\ MPa\ m^{0.5}$ and different hold times. a) t_h = 0.1 h. b) t_h = 1 h. c) t_h = 10 h.

Creep-fatigue crack growth

Figure 4 a) reports CFCG tests performed at a maximum initial nominal value of stress intensity factor amplitude $\Delta K_0 = 21$ MPa m$^{0.5}$ and $\Delta K_0 = 16$ MPa m$^{0.5}$, with different hold times ranging from 0.1 h to 10 h. The results of tests with $\Delta K_0 = 21$ MPa m$^{0.5}$ show the effect of the increasing hold time that significantly reduces the crack propagation rates. Moreover, the test with 0.1 h of hold time is the one performed for comparison on a servo-hydraulic testing machine, where the crack propagation was monitored by means of the elastic compliance method. A relevant difficulty in estimating the crack propagation by means of elastic compliance method was observed for low values of crack length ($a < 0.5$ mm), reflecting in a different trend of the two curves especially in the first stage of the crack propagation. As expected, when comparing the results at the same values of hold time, the crack propagation rates decrease with the initial value of stress intensity factor amplitude.

The experimental values of C_R found by analyzing the experimental load-line deflections, according to the schematic procedure of Figure 1 d), of all the performed experimental tests. Figure 4 b) reports the C_R plotted in as a function of the normalized test time, for the test performed at $\Delta K_0 = 21$ MPa m$^{0.5}$ and hold time $t_h = 2$ h. A stabilized value of C_R was obtained for each experimental test, and an average value for the examined material was found and used in the following CFCG assessments.

The crack tip parameter for creep-fatigue tests under the hypothesis of partial creep reversal may now be calculated according to Equation (1)

$$(C_t)_{avg} = \frac{2\alpha_i\beta_0(1-\nu^2)}{EW} F_{cr}\Delta K^4 \frac{F'}{F}(EA)^{\frac{2}{n-1}}\left[C_R + \frac{2(1-C_R)N^{-\frac{n-3}{n-1}}}{n-1}\right] t_h^{-\frac{n-3}{n-1}} + C^* \qquad (1)$$

where $\alpha_i = 1/(2\pi)[(n+1)^2/(2n\alpha_n^{n+1})]^{2/(n-1)}$ with $\alpha_n^{n+1} = 0.69$ for $3 \le n \le 13$, $\beta_0 = 0.33$ in plane strain conditions, and F_{cr} is a creep angular function.

$(C_t)_{avg}$ is related to the experimental average creep-fatigue crack growth rates as shown in Figure 5 a). The linear relationship through the logarithmic values of $(da/dt)_{avg}$ versus $(C_t)_{avg}$ represents the experimental characterization of the creep-fatigue behavior of the investigated material. This correlation accounts for continuous reinstate of the creep strain at the crack tip under creep-fatigue regime, and addresses the issue to predict CFCG rates in components according to recent creep fatigue ASTM standard [9].

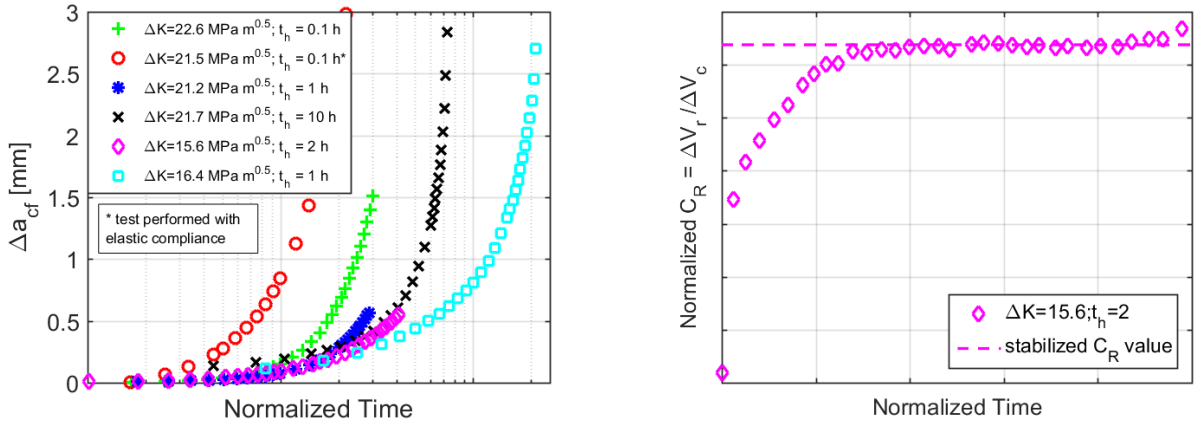

a) *b)*

Figure 4: a) Creep-fatigue crack propagation as a function of time at different initial stress intensity factors and hold times. b) C_R parameter evolution during CFCG test with ΔK_0=15.6 MPa m$^{0.5}$, hold time = 2 h.

The crack propagation per cycle may be expressed as a superposition between a pure fatigue contribution and an additional contribution that includes the effects of creep-fatigue interaction.

$$\frac{da}{dN} = \left(\frac{da}{dN}\right)_{\text{cycle}} + \left(\frac{da}{dN}\right)_{\text{time}} \tag{2}$$

where $(da/dN)_{\text{cycle}}$ is the crack propagation associated to fatigue, according to the Paris-Erdogan law as reported in [10], and the time-dependent contribution may be calculated by the correlation of Figure 5 a).

$$\frac{da}{dN} = C\Delta K^m + t_h D''\left[(C_t)_{avg}\right]^{\phi''} \tag{3}$$

This procedure was included in a Matlab script in order to assess the crack propagation rate during the entire operating life of a component subject to creep-fatigue.

In order to validate the method, the presented model was so far applied to determine CFCG in CT specimens and compare the results with the experimental data. The average fit constants of Figure 5 a) were used to model CFCG according to the $(C_t)_{\text{avg}}$ model defined with the creep reversal parameter. The results in terms of experimental and predicted failure times are summarized in Figure 5 b). The time to failure for the CT specimens is well estimated for each test. For comparison, the CFCG has been also evaluated according to the approach contained in the BS 7910 [11], which is based on a simple superposition model between fatigue and creep crack growth:

$$\frac{da}{dN} = C\Delta K^m + t_h D(C^*)^{\phi} \tag{4}$$

where D and ϕ are material constants fitted to previously performed experimental CCG tests [10].

In this case the experimental rupture times are overestimated for all the tests, and the procedure results generally non-conservative.

After validation with experimental data, the proposed creep-fatigue crack initiation and growth model was extended to the pipe geometry displayed in Figure 6 a) with an initial crack size a = 5%w, at the nominal pressure lof 25 MPa.

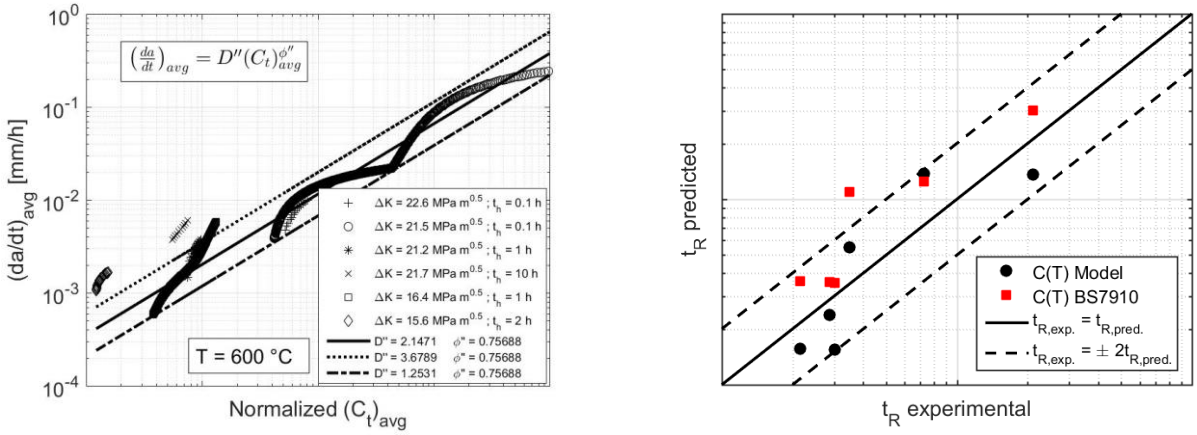

a) *b)*

Figure 5: a) Creep-fatigue average crack propagation rate as a function of the $(C_t)_{avg}$ parameter calculated by assuming the partial reverse of creep strains through the C_R parameter. b) CFCG failure times prediction for CT specimens according to the $(C_t)_{avg}$ approach and the BS 7910

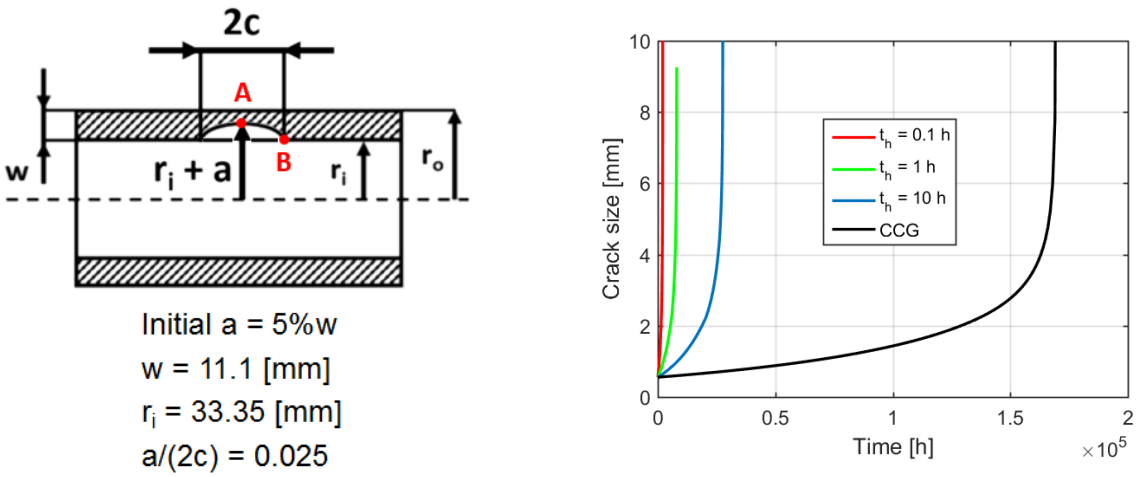

Figure 6: CFCG prediction in a power plant pipe subject to 25 MPa of internal pressure with an initial defect size of 5%w according to the $(C_t)_{avg}$ model.

This initial crack size, may represent an hypothetical defect due to the manufacturing process, or nucleated by accumulation of local high level of creep damage. The C^* parameter of the considered defect ,included in Equation (1), was calculated according to the C_{ref} approach contained in BS 7910 standard [11]. The results shown in Figure 6 b) highlight the detrimental effect given by the cyclic load. The shorter the hold time is, the faster the crack propagation is. However, if a hold time of 10 hours is considered, i.e. the typical operating condition of power plant pipes, the residual life is reduced by an approximated factor of 6 with respect to the life prediction in pure creep crack growth conditions obtained by imposing an infinite hold time.

Conclusion

CFCG tests were performed, on CT specimens of P91 Grade, to assess the effects of different hold times and initial stress intensity factor amplitude on the creep-fatigue crack propagation at the temperature of 600 °C.

Detailed SEM analysis of the fracture surfaces, highlighted the damage interaction mechanisms in terms of accumulation of creep damage and cavitation, eventually assisted by oxidation, and in terms of accelerated linking between microcracks.

The experimental load-line displacement records, were used to estimate the crack tip parameter $(C_t)_{avg}$, that correlates the average crack propagation rates $(da/dt)_{avg}$ and the creep reversal parameter $C_R$that accounts for the interactions between the creep and the cyclic plastic zones allowing an analytical estimation of the $(C_t)_{avg}$ parameter both for specimens and components.

Creep-fatigue crack growth was then predicted for a cracked pipe component, based on experimental results on testing specimens and on the $(C_t)_{avg}$ model. The assessments performed with this method highlighted the detrimental effect of the reduction in the hold time duration on the crack propagation.

Abbreviations

$(C_t)_{ava}$	Crack tip parameter in creep-fatigue conditions
$(da/dt)_{ava}$	Average crack propagation rate in CFCG
$2c$	Semi-elliptical crack shape
α_i	Coefficient in $(C_t)_{ava}$ model
β_0	Coefficient in $(C_t)_{ava}$ model
ΔK	Stress intensity factor amplitude
ΔV_c	Load-line deflection variation during the hold time
ΔV_r	Load-line deflection variation between two adjacent fatigue cycles

ν	Poisson ratio
ϕ'', ϕ	Coefficients in $(da/dt)_{ava}, (da/dt)$ vs. $(C_t)_{ava}, C^*$ relation
A	Norton law multiplier
a	Crack length
C	Paris law multiplier
C^*	Crack tip parameter in steady-state creep conditions
C_R	Creep reversal parameter
C_t	Crack tip parameter valid for small-scale creep
D'', D	Coefficients in $(da/dt)_{ava}, (da/dt)$ vs. $(C_t)_{ava}, C^*$ relation
E	Elastic modulus
F	Shape function
F_{cr}	Creep angular function
$K_{\text{max.0}}$	Maximum initial stress intensity factor
m	Paris law exponent
N	Number of cycles
n	Norton law exponent
P	Applied load
R	Load ratio
r_i	Pipe inner radius
t_h	Hold time
t_R	Rupture time
W	CT specimen or pipe wall thickness

References

[1] M. Speicher, A. Klenk and K. Coleman, "Creep-Fatigue Interactions in P91 Steel," in *13th International Conference on Fracture*, Beijing, China, 2013.

[2] A. Saxena, "Creep Crack Growth Under Nonsteady-State Conditions," *Fracture Mechanics,* vol. ASTM STP 905, pp. 185-201, 1986.

[3] A. Saxena and B. Gieseke, "Transients in Elevated Temperature Crack Growth," in *MECAMAT, International Seminar on High Temperature Fracture Mechanisms and Mechanics III*, 1987.

[4] P. S. Grover, "Creep-fatigue crack growth in Cr-Mo-V base material and weldments," PhD Thesis, Georgia Institute of Technology, 1996.

[5] C. G. Panait, W. Bendick, A. Fuchsmann, A. F. Gourgues-Lorenzon and J. Besson, "Study of the microstructure of the Grade 91 steel after more than 100,000 h of creep exposure at 600 °C," *International Journal of Pressure Vessels and Piping,* vol. 87, no. 6, pp. 326-335, 2010.

[6] Y. Takahashi, "Study on the creep-fatigue evaluation procedures for high-chromium steels-Part I: test results and life prediction based on measured stress relaxation," *International Journal of Pressure Vessels and Piping,* vol. 85, pp. 406-422, 2008.

[7] L. Falat, A. Vyrostkova, V. Homolova and M. Svoboda, "Creep deformation and failure of E911/E911 and P92/P92 similar weld-joints," *Engineering Failure Analysis,* vol. 16, pp. 2114-2120, 2009.

[8] P. S. Grover and A. Saxena, "Modelling the effect of creep-fatigue interaction on crack growth," *Fatigue Fract Engng Mater Struct,* vol. 22, pp. 111-122, 1999.

[9] ASTM A335/A335M - 15a, "Standard specification for seamless ferritic alloy-steel pipe for high-temperature service," ASTM International, 2015.

[10] F. Bassi, S. Foletti and A. Lo Conte, "Creep fatigue crack growth and fracture mechanisms of T/P91 power plant steel," *Materials at High Temperatures,* vol. 32, pp. 250-255, 2015.

[11] American Society for Testing and Materials, "ASTM E2760-10," ASTM International, 2010.

[12] British Standard Institution, BS 7910 Guidance on methods for assessing the acceptability of flaws in metallic structures, 2000.